Increasing Autumn drought over Southern China associated with ENSO regime shift

Article

Published Version

www.reading.ac.uk/centaur

CentAUR

Increasing autumn drought over southern China associated with ENSO regime shift

Wenjun Zhang[1], Fei-Fei Jin[2], and Andrew Turner[3]

[1]Collaborative Innovation Center on Forecast and Evaluation of Meteorological Disasters, Key Laboratory of Meteorological Disaster of Ministry of Education, Nanjing University of Information Science and Technology, Nanjing, China, [2]Department of Meteorology, School of Ocean and Earth Science and Technology, University of Hawaii, Honolulu, Hawaii, USA, [3]NCAS-Climate, Department of Meteorology, University of Reading, Reading, UK
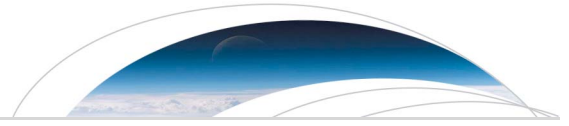
Abstract In the two most recent decades, more frequent drought struck southern China during autumn, causing an unprecedented water crisis. We found that the increasing autumn drought is largely attributed to an ENSO regime shift. Compared to traditional eastern Pacific (EP) El Niño, central Pacific (CP) El Niño events have occurred more frequently, with maximum sea surface temperature anomalies located near the dateline. Southern China usually experiences precipitation surplus during the autumn of EP El Niño years, while the CP El Niño tends to produce precipitation deficits. Since the CP El Niño has occurred more frequently while EP El Niño has become less common after the early 1990s, there has been a significant increase in the frequency of autumn drought. This has implications for increasing precipitation shortages over southern China in a warming world, in which CP El Niño events have been suggested to become more common.

1. Introduction

Autumn is a transitional season from the wet summer monsoon to the dry winter monsoon over China. In autumn, the season for crop maturity and harvest, droughts, and floods invariably cause large economic losses and significant environmental damage. Especially in the most recent two decades, severe autumn droughts have become more frequent over southern China, with catastrophic consequences. For example, the autumn droughts in 2004 and 2009 have left millions of residents suffering water shortages and damaged several million hectares of cropland [*Niu and Li*, 2008; *Zhang et al.*, 2013]. Since the early 1990s, the autumn precipitation over southern China has reduced sharply (Figure 1), consistent with a more frequent occurrence of autumn drought. So far, possible reasons for the decadal decrease of autumn precipitation are unclear, but an understanding of the mechanisms responsible is of importance for future drought management and planning.

It has been demonstrated that the El Niño–Southern Oscillation (ENSO) has a substantial impact on autumn precipitation over China [*Zhang et al.*, 2011; *Wang and Wang*, 2013]. Recent studies reported that a new type of El Niño is observed frequently over the central Pacific (CP), remarkably different from the conventional El Niño whose center of action is confined to the eastern Pacific (EP) [*Larkin and Harrison*, 2005; *Ashok et al.*, 2007; *Kao and Yu*, 2009]. Since the early 1990s, CP El Niño has occurred more often while the EP El Niño has become less common [e.g., *Yeh et al.*, 2009]. For La Niña events, there seems to be no significant change in the zonal location of sea surface temperature (SST) anomalies [*Kug et al.*, 2009; *Ren and Jin*, 2011]. Whether the concurrent decadal change of ENSO regime gives rise to the shift of autumn precipitation over southern China deserves study. This work will discuss possible impacts of the ENSO change on the autumn precipitation over southern China. Our main conclusion is that the decadal decrease in autumn precipitation over southern China is largely attributed to the ENSO regime shift.

2. Data and Methods

The monthly station precipitation data (1961–2010) used here were supplied by the China Meteorological Administration. The Global Precipitation Climatology Centre (GPCC) precipitation data [*Rudolf et al.*, 2005] are also applied to demonstrate consistency of the precipitation anomaly pattern. The SST over the tropical Pacific was used to investigate any decadal shift in ENSO and its links to regional precipitation based on the Hadley Centre sea ice and SST data set [*Rayner et al.*, 2003]. Atmospheric circulation was examined using the National Center for Environmental Prediction/National Center for Atmospheric Research reanalysis data [*Kalnay et al.*, 1996].
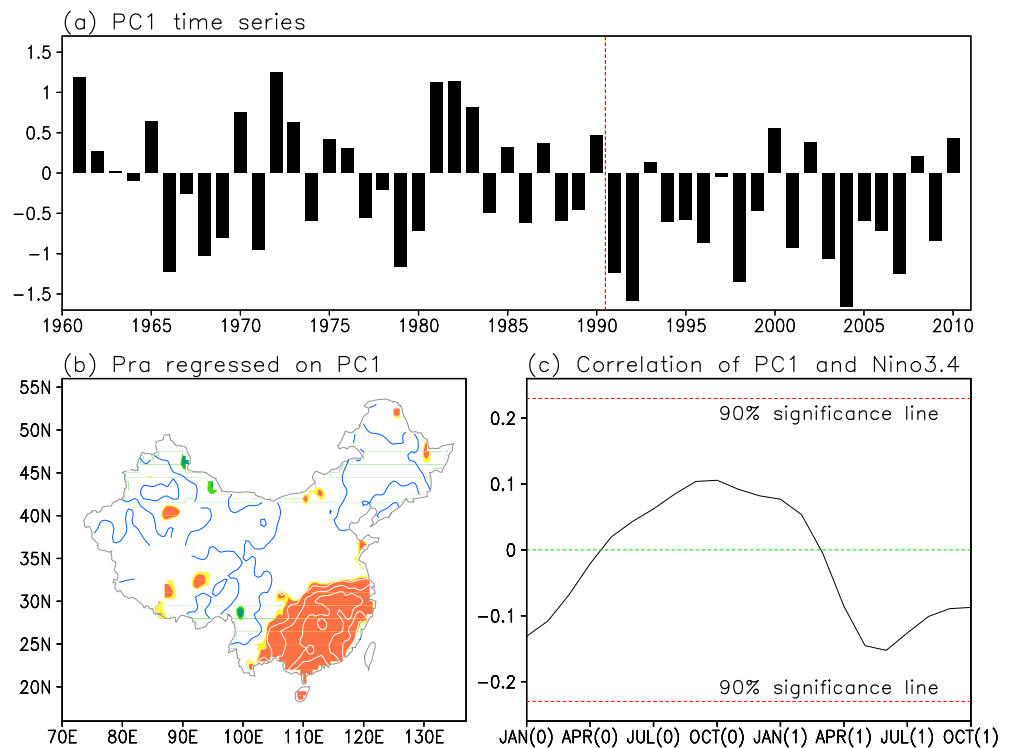
Figure 1. (a) The principal component (PC1) corresponding to the leading mode of SON precipitation for 1961–2010. (b) Precipitation anomalies regressed upon the normalized PC1. The light (deep) shading presents values exceeding the 90% (95%) confidence level. Contours 0.3, 0.5, 0.7, and 0.9 mm/d are added, and blue contours indicate the zero value. (c) The lagged correlation between PC1 and the Niño3.4 SST anomaly in each month from the present year (0) to the following year (1). The red dashed lines indicate values above the 90% confidence level.

Anomalies for all variables were computed as the deviation from the 30 year climatological mean (1961–1990). The climate mean can instead be considered as 1971–2000, with no qualitative impact on the results. In this study, the boreal autumn (September–November (SON)) season is the focus.

Warm and cold episodes are based on a threshold of ±0.5°C for the Niño3.4 region (5°S–5°N, 120°–170°W) SST anomaly from the long-term mean. We identify seven EP El Niño autumns (1963, 1965, 1972, 1976, 1982, 1987, and 1997) and nine CP El Niño autumns (1969, 1977, 1991, 1994, 2002, 2003, 2004, 2006, and 2009) according to the zonal location of SST anomaly and its associated convection described by *Zhang et al.* [2013]. Here La Niña events are classified into one category since there seems no longitudinal change in their maximum cooling, as stated earlier [*Kug et al.*, 2009; *Ren and Jin*, 2011]. These La Niña autumns are 1962, 1970, 1971, 1974, 1975, 1984, 1988, 1995, 1998, 1999, and 2007.

3. Results

Spatial and temporal features in autumn precipitation variability over China are identified by using empirical orthogonal function analysis. The leading principal component (PC1) displays a marked decline of autumn precipitation starting around 1990 (Figure 1a). Based on the moving *t* test technique [*Xiao and Li*, 2007], the decadal abrupt change around 1991 is the most striking and significant (Figure S1 in the supporting information). This decadal signature mainly covers southern China (approximately east of 100°E and south of 32°N), as suggested by the regressed precipitation anomalies (Figure 1b). PC1 well represents autumn precipitation variability over southern China (20°–30°N, 100°–120°E), 85% of whose variance is explained. By examining the PC1 time series, the autumn precipitation over southern China is dominated by interannual variability with oscillations between surplus and deficit years before 1990. Nevertheless, precipitation deficits have become more prevalent after 1990, causing frequent autumn droughts. Therefore, we will present the difference between the periods 1961–1990 and 1991–2010 when analyzing the associated decadal variability hereafter.
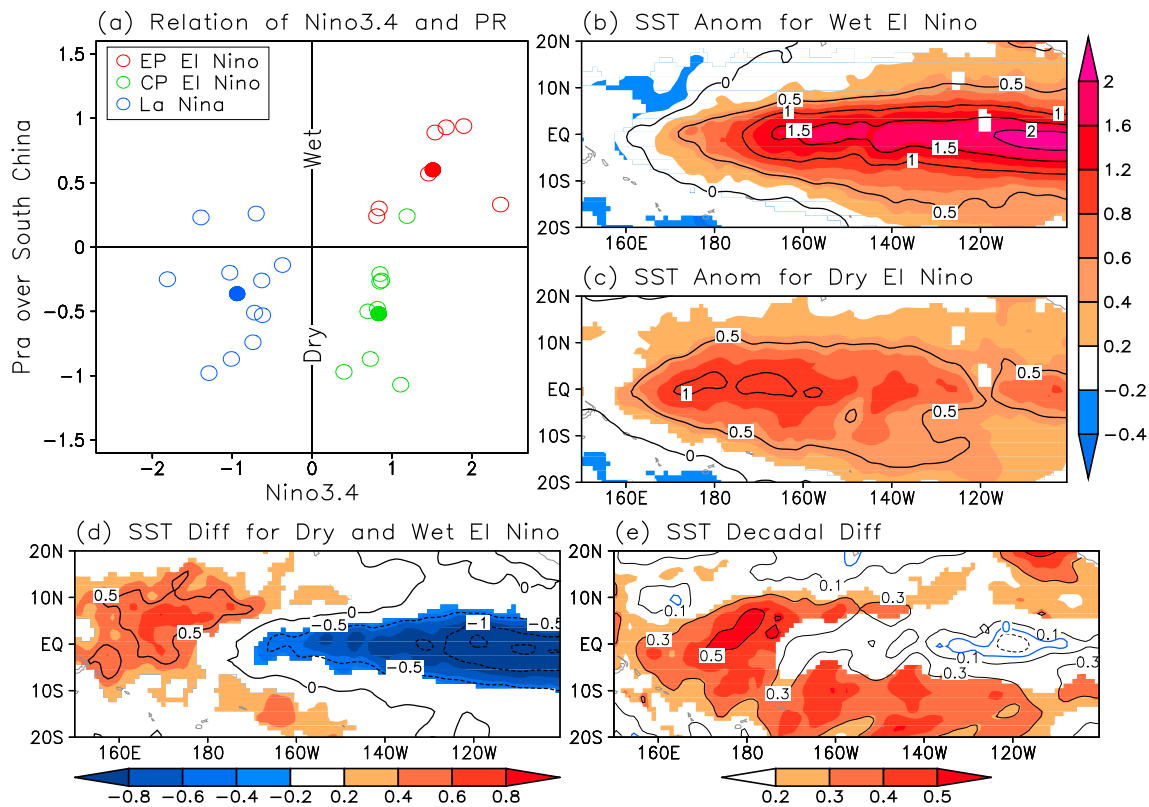
Figure 2. (a) Scatterplot of SON precipitation anomaly (mm/d) over southern China (20°–30°N, 100°–120°E) as a function of SON Niño3.4 SST anomaly (°C) for EP El Niño (red hollow circle), CP El Niño (green hollow circle), and La Niña (blue hollow circle). Solid circles denote composites of different events, whose values exceed 95% confidence level. Composite SST anomalies (°C) of (b) wet and (c) dry El Niño year are shown. (d) Composite SST difference (°C) between dry and wet El Niño years. (e) SST decadal difference (°C) between 1991–2010 and 1961–1990. Contour interval is 0.2 °C, and blue contours indicate zero values. Shading in Figures 2b–2e represents the values above the 95% confidence level.

To detect possible impacts of ENSO on changes in autumn precipitation, Figure 1c shows the lagged correlation between the PC1 time series and Niño3.4 SST anomaly. No significant linear correlation is detected, seemingly indicating that ENSO has no contribution to the autumn precipitation over southern China. We note, however, that only the linear part of such a relationship can be detected in correlation analysis. To avoid overlooking a possible nonlinear relationship, the scatterplot in Figure 2a displays strongly asymmetric responses of autumn precipitation over southern China to ENSO conditions. Autumns with ENSO cold phases usually have precipitation deficits over southern China. However, no simple relationship is detected between the autumn precipitation and Niño3.4 index during El Niño events. Around half the El Niño events are accompanied by increased precipitation (wet El Niño), and the other half are associated with decreased precipitation (dry El Niño). To understand the difference between the El Niño structures, we compute composites of SST anomalies during wet El Niño autumns (top, right quadrant of Figure 2a) and dry El Niño autumns (bottom, right quadrant of Figure 2a), after *Krishna Kumar et al.* [2006] who performed a similar analysis for India. For the wet El Niño, the SST anomaly pattern corresponds to the typical pattern of the EP El Niño featured by the maximum warming in the EP (Figure 2b). In comparison, the dry El Niño displays a warm anomaly focused on the CP with weak EP warming (Figure 2c), which is identified as CP El Niño structure. During these CP warm events, the maximum warming near the dateline is of importance for atmospheric convection because of a high mean state background SST there. Any additional perturbation to this background state can more easily lead to anomalies in convection and diabatic heating overhead [*Turner et al.*, 2005; *Annamalai et al.*, 2007]. The contrasting SST pattern exhibits an east-west dipole over the equatorial Pacific between the dry and wet El Niño events (Figure 2d).

The SST difference in Figure 2d also resembles the mean state equatorial Pacific SST decadal change for the period 1991–2010 minus 1961–1990 (Figure 2e). Relative to the period 1961–1990, the SST is warmer over a horseshoe shape emanating northeast and southeast from the CP during the period 1991–2010. Small
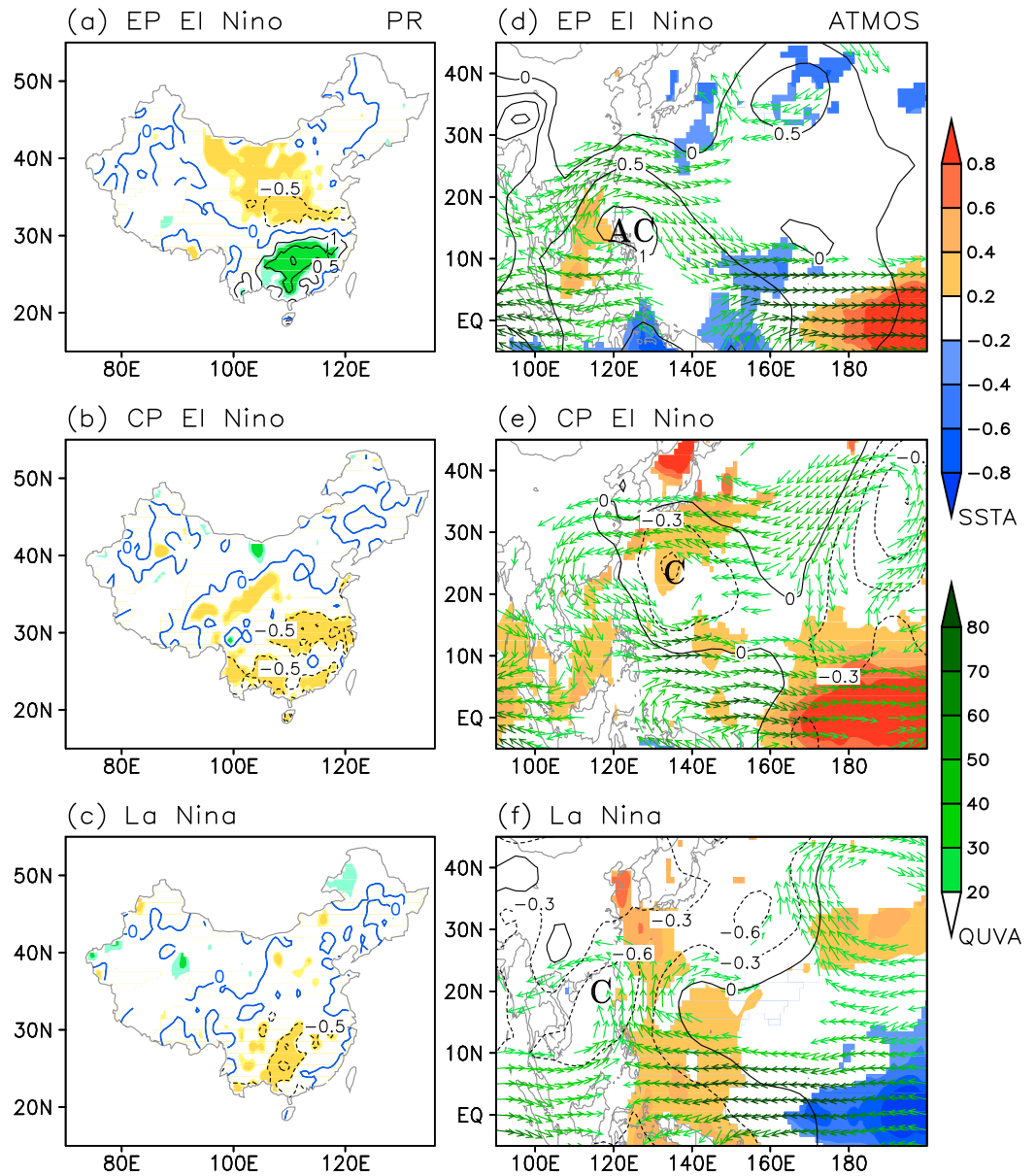
Figure 3. Composites of (left) SON precipitation anomalies (mm/d) and (right) SST anomaly (shading in °C), vertically integrated moisture transport (vector in kg/m/s), and SLP anomaly (contour in hectopascal) for (a, d) EP El Niño, (b, e) CP El Niño, and (c, f) La Niña events. Light (deep) shading in Figures 3a–3c indicates that the anomalies exceeding the 90% (95%) confidence level, and blue contours indicate zero contours. The SST anomalies that are not significant at the 95% level are not shown in Figures 3d–3f. The letters AC and C mark the centers of the anomalous anticyclone and cyclone, respectively.

cooling is observed over the equatorial EP. The similarity between Figures 2d and 2e implies the connection between more CP (dry) and less EP (wet) El Niños and the mean state change over the recent two decades. A recent work also proposed that the tropical Pacific SST decadal change is likely attributed to the asymmetric spatial structures of the CP and EP El Niños [*McPhaden et al.*, 2011].

Since autumn precipitation over southern China is closely associated with ENSO, we use a compositing method to further examine the autumn precipitation responses to different types of ENSO (Figure 3), the years being listed in section 2. During the EP El Niño autumn, a dipolar structure in precipitation anomalies appears over eastern China with deficits over northern China and surplus over southern China (Figure 3a). However, remarkably different precipitation anomalies occur during the CP El Niño autumns (Figure 3b). Southern China experiences almost opposing precipitation anomalies for the two types of El Niño, consistent

with the previous study [*Zhang et al.*, 2011] despite using a slightly different period. These differences in precipitation are associated with roughly opposing atmospheric responses to the two types of El Niño over the western North Pacific (WNP) [*Zhang et al.*, 2011]. During the EP El Niño autumns, an anomalous anticyclone appears over the WNP with a higher-than-normal sea level pressure (SLP) (Figure 3d), in response to the cold SST anomaly over the western Pacific associated with the EP El Niño, as demonstrated by *Wang et al.* [2000]. This anomalous anticyclone transports more moisture to southeastern and eastern Asia and leads to an increase in precipitation over southern China. However, no similar cold SST anomalies are observed during the CP El Niño and the associated CP warming tends to produce an anomalous cyclone over the WNP (Figure 3e), a mechanism supported by a series of idealized modeling experiments in an earlier study [*Zhang et al.*, 2011]. The anomalous WNP cyclone can inhibit the moisture transported northward to China from the south and give rise to less precipitation over southern China. It is thus noted that the teleconnections from ENSO are very sensitive to the zonal locations of the tropical Pacific warming, as in the case for India [*Turner et al.*, 2005; *Krishna Kumar et al.*, 2006; *Annamalai et al.*, 2007]. We note that CP (or Modoki) El Niño events have been further classified into two types (CPI and CPII) according to different impacts over southern China during autumn [*Wang and Wang*, 2013]. The CPII type displays almost the same impacts as that shown in Figure 2b; however, the CPI type shows different impacts, inducing a surplus in central southern China [*Wang and Wang*, 2013]. As shown in Figure 3b, no significant change in precipitation is detected over that region. We caution, though, that further subdividing CP El Nino events here severely limits the sample size available from observations.

For the La Niña autumns, the composited precipitation anomalies display significant precipitation deficits mainly over southern China (Figure 3c). During La Niña autumns, the SST anomaly pattern shown in Figure 3f is almost opposite to that occurring during EP El Niño autumns. Likely as a response to the warming SST anomaly over the western Pacific, an anomalous cyclone emerges over the WNP centered over the South China Sea, which tends to decrease the northward transport of moisture from the south and causes precipitation deficits. Thus, over southern China, the precipitation response to La Niña conditions is similar to that for the CP El Niño and opposite to that for the EP El Niño. The same results are found when using the GPCC precipitation data (not shown). The atmospheric response to CP El Niño is distinct from that to La Niña over the tropical Pacific because of the large difference in the SST anomaly pattern (Figures 3e and 3f). Nevertheless, their associated WNP atmospheric anomalies, directly influencing the local climate over southern China, are similar in spite of some difference in their location and intensity.

To examine the interevent variability associated with different flavors of ENSO, Figure 2a shows a scatter diagram relating Niño3.4 anomaly and autumn precipitation over southern China, marked according to the type of ENSO event. The impact of La Niña on autumn precipitation over southern China is relatively stable over the past five decades. During about 82% (9 of 11) of the La Niña autumns, precipitation deficits appear over southern China, where the precipitation is reduced by about 0.4 mm/d on average. During all seven EP El Niño autumns, southern China experiences a precipitation surplus with an average anomaly of 0.6 mm/d. Approximately 89% (8 of 9) of the CP El Niño autumns are accompanied by the precipitation deficits averaging 0.5 mm/d over southern China. Each of the two flavors of El Niño exhibits a high consistency in its impact on autumn precipitation over southern China.

As indicated in Figure 2, many studies have identified that El Niño events exhibit a decadal change in their zonal location since 1990, whereas no significant change is known in La Niña events [e.g., *Kug et al.*, 2009; *Ren and Jin.*, 2011]. Since regional precipitation patterns described above have been shown as sensitive to the location of the warm SST anomaly and ultimately the warmest absolute SST values, the ENSO regime change over recent decades leads to a change in autumn precipitation change over the same period. Figure 4a shows the time series of autumn precipitation anomalies over southern China relative to the timing of the various ENSO events. In the pre-1990 period, ENSO warm events are dominated by EP El Niños (red dots), which cause more precipitation over southern China including four severe wet events (anomalies exceeding 1 standard deviation). After 1990, the El Niño mainly consists of the CP type (green dots), inhibiting autumn precipitation over southern China with four severe droughts. La Niña events (blue dots) remain unchanged in their impacts on autumn precipitation in these two periods. Therefore, the ENSO regime change occurring around 1990 (i.e., more CP El Niño and fewer EP El Niño events) gives rise to more frequent recurrent autumn precipitation deficits over southern China.

To further investigate its decadal pattern, Figures 4b and 4c show the decadal differences of autumn precipitation between 1961–1990 and 1991–2010. Over eastern China, the autumn mean state precipitation
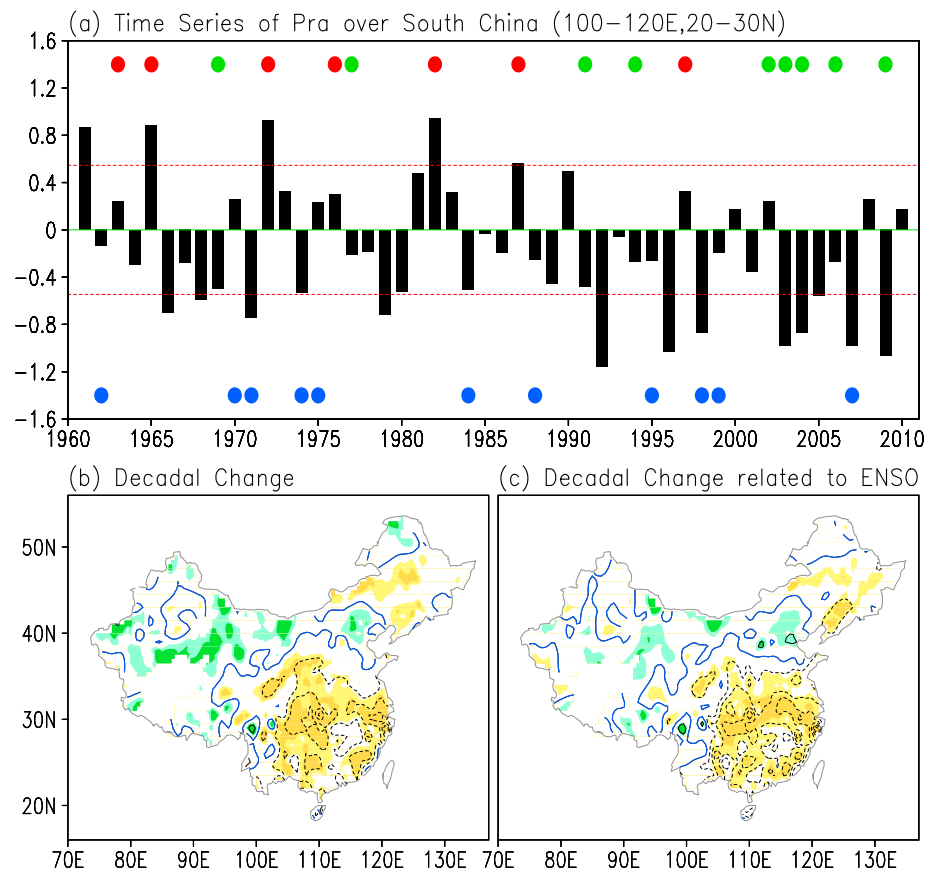
Figure 4. (a) Time series of SON precipitation anomalies (mm/d) over southern China (20°–30°N, 100°–120°E). The red lines represent 1 standard deviation. Red, green, and blue dots denote the EP El Niño, CP El Niño, and La Niña events, respectively. (b) Total decadal difference of SON precipitation (mm/d) between 1991–2010 and 1961–1990. (c) Decadal difference of SON precipitation (mm/d) associated with ENSO events between 1991–2010 and 1961–1990. Light (deep) shading indicates values exceeding 90% (95%) confidence level. The contour interval in Figures 4b and 4c is 0.3 mm/d, and blue contours denote zero values.

significantly decreases after 1990, especially in the middle and lower reaches of the Yangtze River valley and southwestern China (Figure 4b). In order to evaluate the ENSO contribution to the decadal change, we display the autumn precipitation differences associated with ENSO events in these two periods (Figure 4c). The ENSO-related precipitation differences are obtained through the average precipitation anomalies during all El Niño and La Niña autumns in 1991–2010 minus those in 1961–1990. The precipitation difference patterns associated with ENSO are very similar to the total decadal difference, suggesting that the decadal changes in autumn precipitation over southern China are most likely related to the ENSO change in its spatial structure as shown earlier in Figures 2d and 2e.

4. Conclusion and Discussion

Southern China experienced a significant decadal change in autumn precipitation with increasingly frequent droughts after the early 1990s. Meanwhile, ENSO also exhibited a robust change in its zonal location for warm events over the same period. There has been an increase in the frequency of CP El Niño with SST anomalies centered over the central equatorial Pacific while EP El Niño has become less common. We show that autumn precipitation responses over southern China are very sensitive to the zonal location of El Niño. The EP El Niño leads to precipitation surplus, whereas CP El Niño tends to produce precipitation deficits over southern China during autumn. Instead, La Niña displays a relatively high stability in its impacts on the autumn precipitation over southern China accompanied by precipitation deficits. Since the CP El Niño has become a dominant mode of ENSO warm phase versus

the EP El Niño after 1990, the autumn drought becomes more frequent over southern China. Therefore, the ENSO regime shift is largely responsible for the decadal decrease of autumn precipitation over southern China.

It is notable that the Pacific Decadal Oscillation (PDO) index [*Zhang et al.*, 1997; *Mantua et al.*, 1997] also shows a phase transition around the early 1990s (Figure S2), apparently coincident with the decadal shift of autumn precipitation over southern China. However, when the PDO experienced another significant phase transition around the late 1970s, no analogous decadal change was detectable for autumn precipitation over southern China. Moreover, no significant correlation is detected between the PDO and decadal-mean autumn precipitation over southern China over the period 1961–2010 (Table S1). We also show in Figure S3 the SST decadal difference between 1961–1990 and 1991–2010, the transition period defined in this study. No PDO-like SST anomalies are observed in the North Pacific. These results suggest that the PDO does not play a major role in the decadal change of the autumn precipitation over southern China.

At present, the mechanisms that are driving more CP El Niño events at the expense of EP El Niño events are not clear. Some studies have proposed that the background state could modulate ENSO spatial structures [*Yeh et al.*, 2009; *Xiang et al.*, 2013]. Other studies suggest that the residuals caused by spatial irregularity associated with the two types of El Niño make a contribution to the change in the background mean state [e.g., *McPhaden et al.*, 2011]. This relationship between ENSO and the mean state remains poorly understood, although some progress has been made based on models [e.g., *Guilyardi*, 2006]. *Yeh et al.* [2009] argued that there is a possible increased occurrence of the CP El Niño with global warming. If so, the autumn drought will become more and more frequent over southern China under future greenhouse warming, with potential for a disaster in regional ecosystems.

References

Annamalai, H., K. Hamilton, and K. R. Sperber (2007), The south Asian Summer Monsoon and its relationship with ENSO in the IPCC AR4 simulations, *J. Clim.*, *20*, 1071–1092.

Ashok, K., S. K. Behera, S. A. Rao, H. Y. Weng, and T. Yamagata (2007), El Niño Modoki and its possible teleconnection, *J. Geophys. Res.*, *112*, C11007, doi:10.1029/2006JC003798.

Guilyardi, E. (2006), El Niño-mean state-seasonal cycle interactions in a multi-model ensemble, *Clim. Dyn.*, *26*, 329–348.

Kalnay, E., et al. (1996), The NCEP/NCAR 40-year reanalysis project, *Bull. Am. Meteorol. Soc.*, *77*, 437–471.

Kao, H. Y., and J. Y. Yu (2009), Contrasting eastern-Pacific and central-Pacific types of ENSO, *J. Clim.*, *22*, 615–632.

Krishna Kumar, K., B. Rajagopalan, M. Hoerling, G. Bates, and M. Cane (2006), Unraveling the mystery of Indian monsoon failure during El Niño, *Science*, *314*, 115–119.

Kug, J. S., F. F. Jin, and S. I. An (2009), Two types of El Niño events: Cold tongue El Niño and warm pool El Niño, *J. Clim.*, *22*, 1499–1515.

Larkin, N. K., and D. E. Harrison (2005), On the definition of El Niño and associated seasonal average U.S. weather anomalies, *Geophys. Res. Lett.*, *32*, L13705, doi:10.1029/2005GL022738.

Mantua, N. J., S. R. Hare, Y. Zhang, J. M. Wallace, and R. C. Francis (1997), A Pacific interdecadal climate oscillation with impacts on salmon production, *Bull. Am. Meteorol. Soc.*, *78*, 1069–1079.

McPhaden, M. J., T. Lee, and D. McClurg (2011), El Niño and its relationship to changing background conditions in the tropical Pacific Ocean, *Geophys. Res. Lett.*, *38*, L15709, doi:10.1029/2011GL048275.

Niu, N., and J. P. Li (2008), Interannual variability of autumn precipitation over South China and its relation to atmospheric circulation and SST anomalies, *Adv. Atmos. Sci.*, *25*, 117–125.

Rayner N. A., D. E. Parker, E. B. Horton, C. K. Folland, L. V. Alexander, D. P. Rowell, E. C. Kent, and A. Kaplan (2003), Global analyses of sea surface temperature, sea ice, and night marine air temperature since the late nineteenth century, *J. Geophys. Res.*, *108*(D14), 4407, doi:10.1029/2002JD002670.

Ren, H.-L., and F.-F. Jin (2011), Niño indices for two types of ENSO, *Geophys. Res. Lett.*, *38*, L04704, doi:10.1029/2010GL046031.

Rudolf, B., C. Beck, J. Grieser, and U. Schneider (2005), Global precipitation analysis products, Global Precipitation Climatology Centre (GPCC), DWD, Internet publication, 1–8.

Turner, A. G., P. M. Inness, and J. M. Slingo (2005), The role of the basic state in the ENSO-monsoon relationship and implications for predictability, *Q. J. R. Meteorol. Soc.*, *131*, 781–804.

Wang, C., and X. Wang (2013), Classifying El Niño Modoki I and II by different impacts on rainfall in Southern China and Typhoon Tracks, *J. Clim.*, *26*, 1322–1338.

Wang, B., R. Wu, and X. Fu (2000), Pacific-East Asian teleconnection: How does ENSO affect East Asian Climate?, *J. Clim.*, *13*, 1517–1536.

Xiang, B., B. Wang, and T. Li (2013), A new paradigm for predominance of standing Central Pacific Warming after the late 1990s, *Clim. Dyn.*, *41*, 327–340.

Xiao, D., and J. Li (2007), Spatial and temporal characteristics of the decadal abrupt change of global atmosphere–ocean system in the 1970s, *J. Geophys. Res.*, *112*, D24S22, doi:10.1029/2007JD008956.

Yeh, S. W., J. S. Kug, B. Dewitte, M. H. Kwon, B. P. Kirtman, and F. F. Jin (2009), El Niño in a changing climate, *Nature*, *461*, 511–514.

Zhang, Y., J. M. Wallace, and D. S. Battisti (1997), ENSO-like interdecadal variability: 1900–93, *J. Clim.*, *10*, 1004–1020.

Zhang, W., F.-F. Jin, J. Li, and H.-L. Ren (2011), Contrasting impacts of two-type El Niño over the western North Pacific during boreal autumn, *J. Meteorol. Soc. Jpn.*, *89*, 563–569.

Zhang, W., F.-F. Jin, J. X. Zhao, L. Qi, and H.-L. Ren (2013), The possible influence of a non-conventional El Nino on the severe autumn drought of 2009 in Southwest China, *J. Clim.*, *26*, 8392–8405.